THERMAL ANALYSIS OF SHELL-SIDE FLOW OF SHELL-AND TUBE HEAT EXCHANGER USING EXPERIMENTAL AND THEORETICAL METHODS

S. Noie Baghban, M. Moghiman and E. Salehi

Department of Chemical Engineering, Ferdowsi University of Mashhad
Mashhad, Iran

(Received: October 1, 1998 - Accepted in Revised Form: June 3, 1999)

Abstract In this paper the thermal behavior of the shell-side flow of a shell-and-tufe heat exchanger has been studied using theoretical and experimental methods. The experimental method Provided the effect of the major parameters of the shell-side flow on thermal energy exchange. In the numerical method, besides the effect of the major paramerers, the effect of different geometric parameters and Re on thermal energy exchange in shell-side flow has been considered. Numerical analysis for six baffle spacings namely 0.20, 0.25, 0.33, 0.50, 0.66, and 1.0 of inside diameter of the shell and five baffle cuts namely 16%, 20%, 25%, 34%, and 46% of baffle diameter, have been carried out. In earlier numerical analyses, the repetition of an identical geometrical module of exchanger as a calculation domain has been studied. While in this work, as a new approach in current numerical analysis, the entire geometry of shell-and-tube heat exchanger including entrance and exit regions as a calculation domain has been chosen. The results show that the flow and heat profiles vary alternatively between baffles. A shell-and-tube heat exchanger of gas-liquid chemical reactor system has been used in the experimental method. Comparison of the numerical results show good agreement with experimental results of this research and other published experimental results over a wide rang of Reynolds numbers (1,000-1,000,000).

Key Words Heat Exchanger, Shell-Side Flow, Baffle Cut, Baffle Space.

º B´ { °n pA ²j B´ TwA B¥ ³§±§ ° ³Tw±Q »¥nkoe ¤kL« ð ½ ³Tw±Q ¬°nj ¬B½o] »¥nkoe nBTµn ³§B¸« Ë½A nj **²k¼ña**
Baffle Space :¬¬jo¢¥C ¨B£ S§Be y { ºko¥ ºjkî ¥¼¦dU /SwA ³TµoE nko¹ ³ í§B¤« ° »wno¥ jn±« ºjkî ° »¥lo \ U
Baffle Cut (bc) = 0.16 0.20 0.25 0.34 :¬¬jo¢¥C »£k½o¥ S§Be [®Q °(bs) = 0.20-0.25-0.33-0.50-0.66
/k¼²k{ ³v½B¸« ©µ B¥ 1000000 B¥ 1000 pA ³ ¦Th« pk§±®½n jAkîA ºko¥ ºjkî ° »¥lo \ U [½BT ° ³TµoE ¨B \ ¯A -0.46
¬¬±®î ³¥ ,¬B½o] º±¢§A o¥ »] °o i ° ºj°n° · ¥B®« RkoYA ËTµoE o¨¨ nj ° ³Tw±Q ¥ i Aj ¬B½o] ¥«B½ »wno¥ ºko¥
ºjkî x °n ³LwBd« ²p±e ¬¬±®î ³¥ º A³ ¼±TwA ¤kL« »ñ½q¼µ ²p±e ¨BªU ºjkî ¨±wo« ºB´ {°n nj k½k] nB½ ð ½
³ªza ° S½oe n¬k¸« ³§jBí« nj ©T®«±« ²Ba Rn±æ ³¥ ¤kL« ºBµ³§±§ »¥nkoe ° »½Bñ¤æA RkoYA ° ²k{ J Bh T¯A
J °B®ÇU ²k ç«C Swj ³ÇW [½BT¯ /SwA ²k{ ³Tµo£ o¨¨ nj ,k¯n¬j j±] ° Bµ³§±§ ³½ »¥B¸¯ nj ºro¯A ³§jBí« nj »¥nkoe
nj ³½ ³§±§ ° ³Tw±Q »¥nkoe ¤kL« ð ½ pA »¥lo \ U x °n nj /kµj»« ¬Bz¯ »¥¥± i ³¥ ¬n B´ ¬A jo¢¥C Ë¼W »¥nkoe ° »¯B½o]
ËÇ¬A »¥lo \ ÇU [½BT¯ B¥ ²k«C Swj ³¥ ºjkî [½BT¯ /SwA ²k{ ²jB´ TwA ,jn¬j nko¹ é½B« Ç pB£ »½B¼ª¼{ n±T½¼n 4¥ñ¼w
nj ³Ç½ kµj»Ç« ¬Bz¯ [½BT¯ /kµj»« ¬Bz¯ ¬n »¥¥±¤« · µ¬±U ³½ SwA ²k{ ³v½B¸« ¬¬o¢½j »¥lo \ U [½BT¯ ° y µ°sQ
/k{B¥»« ¬¬jo¢¥C »£k½o¥ oYA pA oTª´« ¬¬jo¢¥C ¨B£ oYA ³§±§ ° ³Tw±Q ºB´ §kL« ¥ i Aj S½oe ¤B¸T¯A k®¼¼oµ

INTRODUCTION

Shell-and-tube heat exchangers are used in many thermal industries [1]. Their proper designs play a vital role in heat recovery and increase the efficiency of industrial cycles. The shell-side flow has the greatest effect on the efficiency of exchanger. An appropriate shell-side flow can increase heat transfer and reduce the pressure drop and pumping expenses. The behavior of this complex flow is

severely affected by parameters such as baffle spacing, baffle cut, Re and Pr of the fluid. Inappropriate selection of each of the above-mentioned parameters may create problems such as reduction of cross-sectional area, creation of wide vortex regions, reduction of heat transfer and increase of pressure drop. Tinker [2] examined more than 75 cases of different geometric parameters. However, due to problems prevailing in laboratory experiments, he managed to analyze only a few limited cases of baffle spacing and baffle cut. Patankar and Spalding [3] carried out numerical analyses using three dimensional models with a prosmatic shell for two baffles only. They mentioned that due to the problems existing at the time they were unable to vary baffle numbers or other variables. Other investigators [4,5,6] have based their work on the model with one or more baffles restricted by two flat plates on the top and bottom. They assumed that the primary inlet flow was always parallel to the plate. This assumption is in direct contrast with real flows in exchangers.

Previous works have revealed that experimental analyses face the problem of measurement of detail thermal and hydrodynamic conditions of shell-side flow Numerical analysis has been carried out only for a part of exchanger as a geometrical module with fully developed flow. In this way, the effect of inlet and outlet conditions do not appear in calculations [5,6]. while in the present research, the entire geometry of the shell-and-tube heat exchanger has been considered.

In this investigation the first experimental tests were conducted on a shell-and-tube heat exchanger. The experimental results have been used for validating numerical analysis. The shell-side heat transfer coefficient has been obtained by varying Reynolds number of shell-side flow (changing the inlet flow rate), and measuring inlet-outlet fluid temperatures. By comparing the theoretical and experimental results, the theoretical model used in calculations for prevailing exchanger conditions was validated. The influence of other baffle cases on heat transfer rate has been investigated using theoretical models.

GEOMETRICAL CHARACTERISTICS OF THE HEAT EXCHANGER

The heat exchanger used in the experimental test was a part of a chemical reactor system [7]. The schematic diagram of the reactor system is shown in Figure 1. Thermal design of the heat exchanger was based on Kern's Method [8] and its mechanical design and construction on the TEMA standard [9]. The material used in all parts of the heat exchanger was SS-316. It had four segmental baffles. All tubes were seamless. The rig was equipped with instruments - Bourdon pressure gauge (accurate to $\times 0.5$ psi), Bourdon temperature gauge (accurate to $\times 1$K) and Rotameter (accurate to $\times 0.5$ lit) for measuring temperature, pressure and flow rate - in different parts of the heat exchanger. The end views of a tube sheet and the baffle are shown in Figures 2 and 3 respectively. Other geometric characteristics of exchanger are as follows:

t=0.01 m	ID_s=0.86 m	N=121	
A=7.6 m^2	PT/OD_t=1.5	L=1 m	
q=130 kw	OD_t=0.02 m	bc=25%	
bs=0.195 m	ID_t=0.016 4m	m=1	n=1

THE GOVERNING EQUATIONS

The equations which govern the turbulent flow inside the shell of the heat exchanger are conservation of mass, momentum and energy.

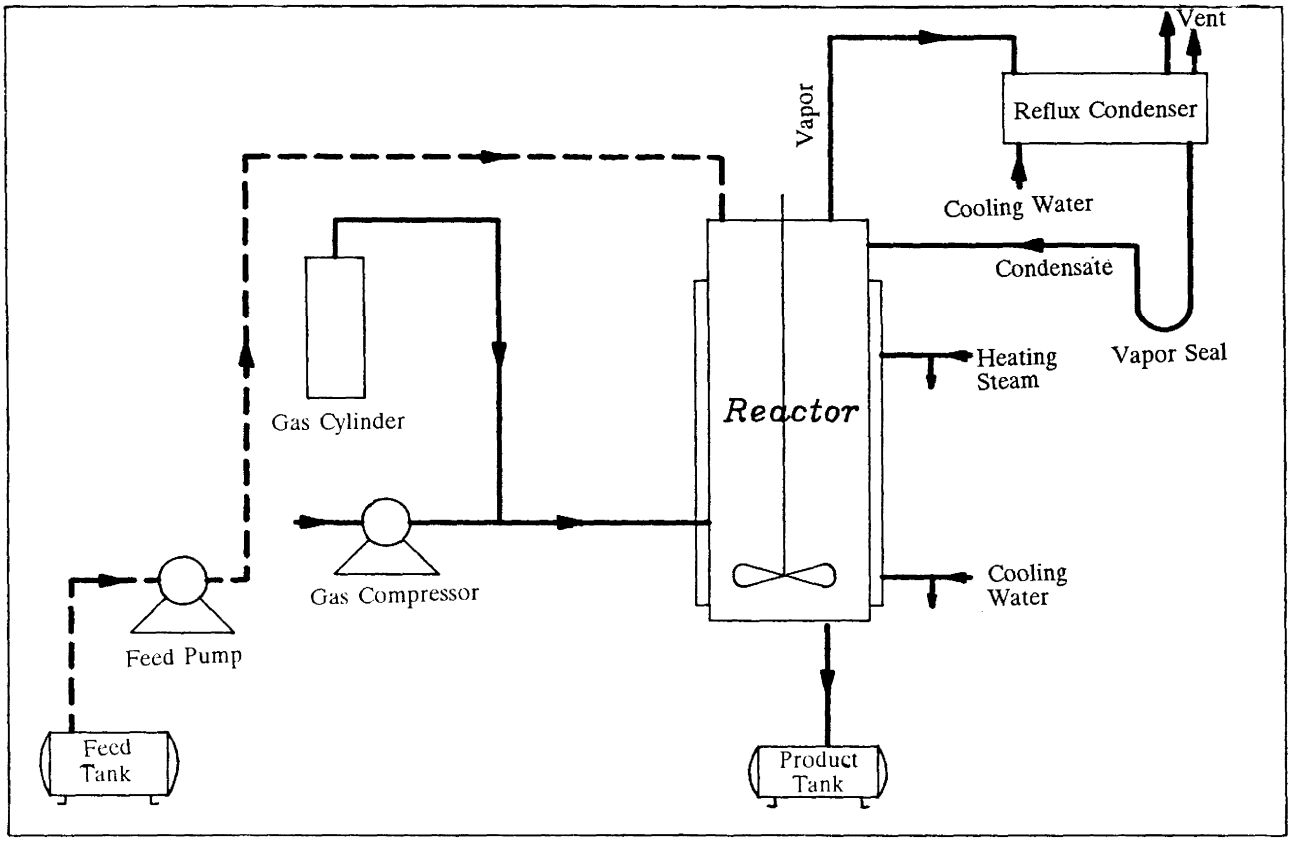

Figure 1. Schematic diagram of the reactor system.

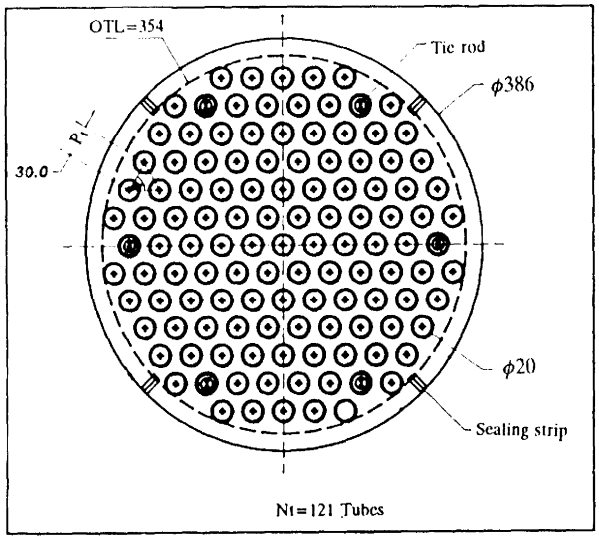

Figure 2. Reflex condenser tube sheet view.

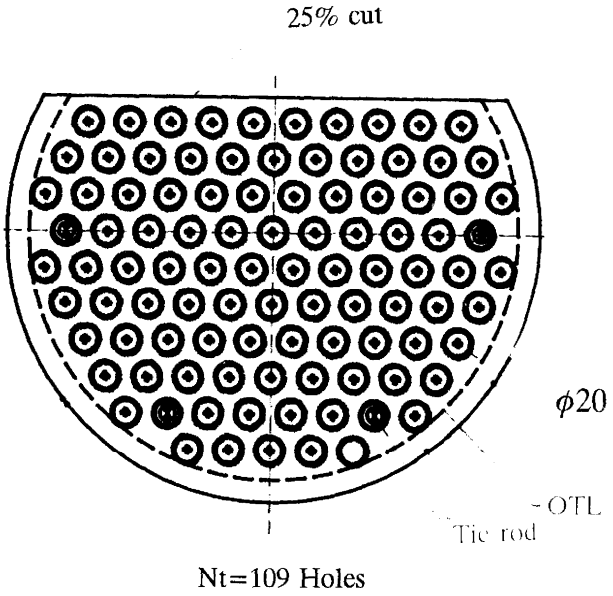

Figure 3. Reflux condenser baffle view.

These equations written in cylindrical co-ordinates are as follows [10]:

a) The continuity equation:

$$\frac{\partial}{\partial x}(\beta \rho u) + \frac{1}{r}\frac{\partial}{\partial r}(r \beta \rho v)=0$$

b) x-direction momentum equation:

$$\frac{1}{\beta}\left[\frac{\partial}{\partial x}(\beta\rho u^2) + \frac{1}{r}\frac{\partial}{\partial r}(r \beta \rho v u)\right] = -\frac{\partial p}{\partial r} - \frac{\partial}{\partial x}(r\beta\rho uv) - \frac{\partial}{\partial x}(r\beta\mu u) + R_x$$

c) r-direction momentum equation:

$$\frac{1}{\beta}\left[\frac{\partial}{\partial x}(\beta\rho uv) + \frac{1}{r}\frac{\partial}{\partial r}(r \beta \rho v^2)\right] = -\frac{\partial p}{\partial r} - \frac{\partial}{\partial x}(r\beta\mu uv) - \frac{1}{r}\frac{\partial}{\partial x}(r \beta \rho vv) - \frac{1}{r} r \rho ww + R_r$$

where β is the porosity defined as the ratio of the volume occupied by the fluid to the total (nominal) value. R_x and R_v are frictional resistance of tube to flow which are expressed as:

$$R_x = -2f_x \rho u G/ (\rho D_h)$$

where:

$$f_x = 0.048 (G D_h / \mu)^{-0.2}$$

$$R_r = 2f_r G_{max} G/ (\rho P_T)$$

where:

$$f_r = [0.23 + 0.11/ (\sqrt{3}P_T/OD_t)^{1.08}] (G OD_{t/\mu})^{-0.15}$$

d) The energy equation:

$$\frac{1}{\beta}\left[\frac{\partial}{\partial x}(\beta\rho uh) + \frac{1}{r}\frac{\partial}{\partial r}(r \beta \rho vh)\right] = \frac{\partial}{\partial x}\left(\Gamma_h \beta \frac{\partial h}{\partial x}\right) + \frac{1}{r}\frac{\partial}{\partial r}\left(r\beta\Gamma_h \frac{\partial h}{\partial r}\right) + S_h$$

where S_h is the rate of heat transfer per unit volume of the shell fluid and has to be calculated from experimental data.

The effect of the presence of the tube in the shell-side flow is included in two different ways. The first effect of the tubes is that they provide distributed resistance to flow, thus producing a distributed "sink" for momentum. The second effect is that they produce source of heat. These effects of tubes are introduced into calculations through the momentum and energy in the above equations.

e) The equation of turbulent kinetic energy (k) and its dissipation rate (ε):

In view of the disability of the k-ε model to cope with anisotropic flows [11,12], the turbulent stresses are obtained from an algebraic stress model [13]. In this model in addition to the six algebraic relations it is necessary to solve the equation for transport of kinetic energy of turbulence and its dissipation rate.

$$\frac{1}{\beta}\left[\frac{\partial}{\partial x}(\rho uk) + \frac{\partial}{\partial r}(\rho vk)\right] = \frac{1}{r}\left[\frac{\partial}{\partial r}\left(r\frac{\Gamma_k}{\sigma_k}\frac{\partial k}{\partial r}\right) + \frac{\partial}{\partial x}\left[\frac{\Gamma_k}{\sigma_k}\frac{\partial k}{\partial x}\right] + G_k - \rho\varepsilon\right]$$

$$\frac{1}{\beta}\left[\frac{\partial}{\partial x}(\rho u\varepsilon) + \frac{\partial}{\partial r}(\rho v\varepsilon)\right] = \frac{1}{r}\frac{\partial}{\partial r}\left[r\frac{\Gamma_\varepsilon}{\sigma_\varepsilon}\frac{\partial \varepsilon}{\partial r}\right] + \frac{\partial}{\partial x}\left[\frac{\Gamma_\varepsilon}{\sigma_\varepsilon}\frac{\partial \varepsilon}{\partial x}\right] + C_1\frac{\varepsilon}{k}G_k - C_2\rho\frac{\varepsilon^2}{k}$$

where:

$C_1= 1.44$ $C_2= 1.92$ $\sigma_k=1$ $\sigma_\varepsilon=1.3$ [14]

NUMERICAL SOLUTION AND BOUNDARY CONDITIONS

The heat exchanger is divided in a 192*48 grid (axial * radial) in a non-uniform manner with closer grid lines in regions of steep velocity gradients (Figure 4). The governing Partial differential equations for the conservation of mass, momentum, stagnation enthalpy, turbulence energy and its dissipation rate are reduced to their discretisation equations by integration over the computational cells into which the domain of interest is subdivided [15].

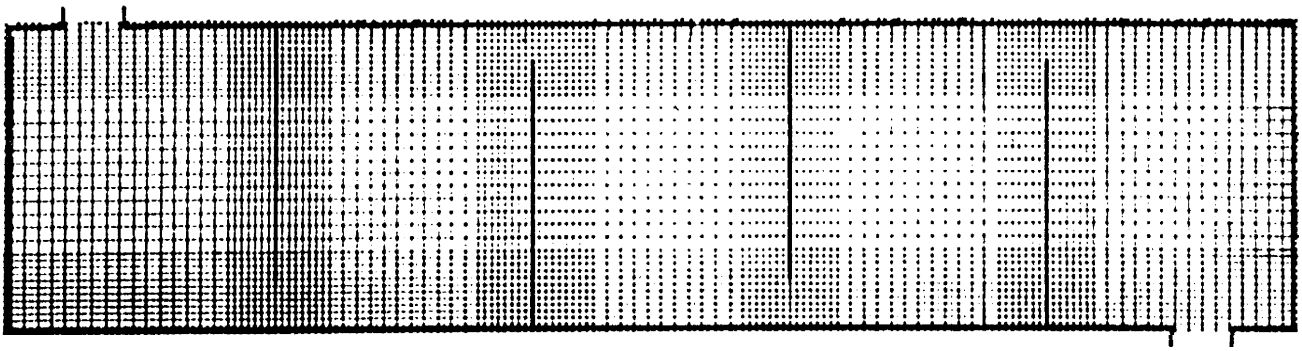

Figure 4. Calculation domain.

The resulting algebraic equations can be given in the following common form:

$$\sum_{i=N,S,E,W} (A_i - S_p)\, f_p = \sum_{i=N,S,E,W} A_i\, f_i + S_u$$

where f represents the general dependent variable, the A's are the coefficients which contain contributions from the convective and diffusive fluxes, S_u and $S_p f$ are the linearised source terms. Power law scheme is used tocalculate the diffusion and convection terms. The set of simultaneous algebraic equations are solved by a semi-implicit iterative technique [15]. Because of the elliptic nature of the conservation equations, a complete description of the flow field considered necessitates the specification of boundary conditions at all boundaries of the domain of interest. Theboundary conditions at the inlet are specified once for all. At the exit plane the conditions are know beforehand and it is assumed that the radial gradients of all the variables vanish on this plane. In the regions near solid boundaries, where the variations in the dependent variables may be very sharp, the outer solutions are matched by well-established wall functions [14].

The specific wall functions employed in this study are:

$$(\frac{t}{r})_w = u_{nw} (k_{nw} C_m^{1/2})^{1/2} [\frac{1}{x} \ln (E \frac{k_{nw} C_m^{1/2}}{v} y_{nw})]$$

$$e_{nw} = (k_{nw} C_m^{1/2})^{3/2} / x y_{nw}$$

where t is the shear stress at the wall, u_{nw}, k_{nw} and e_{nw} are velocity, turbulence energy and disspation rate at a normal distance y_{nw} from the wall, x, E and C_m are constants which are given the values, 0.4187, 9.793 and 0.09 respectively. The subscripts w and nw denote the locations on and near the wall.

The friction and thermal effects of tubes have been taken into account as a momentum sink in the momentum equation and heat source in the energy equation.

EXPERIMENTAL RESULTS

After several tests, the temperatures and flow rates on inlet and outlet fluid were measured. Typical results are as follows:

Inlet temperature of saturated steam in tubes	418 K
Outlet temperature of saturated liquid in tubes	418 K
Inlet temperature of water inside shell	290 K
Outlet temperature of water inside shell	302 K
Flow rate of water inside shell	40lit/min

The experimental and theoretical results of this research were compared with those of other investigators namely Tinker [2], Kern [8] and Bell [6]. This comparison is shown in Figure 5 in the form of dimensionless heat transfer, J_h, over a wide range of Reynolds numbers (1,000 to

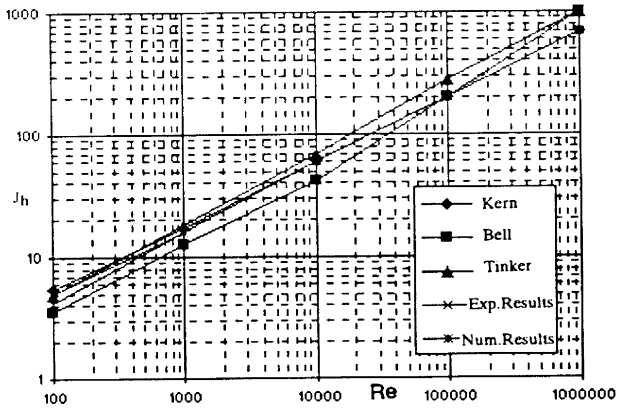

Figure 5. Heat transfer coefficient.

1,000,000). The small deviation between the curves are well within the range of experimental error, which is due to differences in the models used by different investigators.

THEORETICAL RESULTS

With regards to the satisfactory results obtained form the comparison between theoretical and experimental results on the entire field of shell-side flow, in this section the role of baffles on the flow and the temperature profile have been investigated by numerical methods.

Temperature Profile in Exchanger without Baffles Initially, an exchanger without baffles was analysed as a base condition. Figure 6-A shows streamlines inside the exchanger without baffles. As can be observed, a wide field of vortex flow is caused on the top of the exchanger. Figure 6-B shows the temperature profile inside the shell in the form of isothermal lines. It has been observed that due to the absence (disuse) of baffles and consequently creation of wide vortex and trap of a large part of fluid inside the shell, the fluid temperature in this section increases considerably. However, the rest of the flow inside the shell leaves the exchanger in a short path and parallel to tubes without causing considerable temperature change. In other words, the entire exchanger has not been uniformly used for optimal heat exchange.

Temperature Profile in Exchanger with Baffles There is no exact selection for baffle spacing and baffle cut for optimal conditions in practical situations. Only baffle spacing in the range of 0.2 to 1.0 and baffle cut in the range of 15% to 50% have been indicated. Hence, in this research, six baffle spacings (bs= 0.20, 0.25, 0.35, 0.50, 0.66, 1.0) and five baffle cuts (bc= 16%, 20%, 25% 34%, 46%) have been analysed numerically.

The streamlines for bs= 0.33 and three baffle cuts are shown in Figure 7. In this figure a wide vortex field observed in Figure 6-A has disappeared and the flow passes a longer distance. In other words, the entire volume of the exchanger has been properly uses and only in the corners and behind the base of the baffles, small regions of vortex are detectable. In Figures 8 and 9 the isothermal lines for two baffle spacings and five baffle cuts are drawn. An analysis of these figures shows that:

a) In the region with high vortex motion and low translation motion, the temperature increases locally and on the edge of baffles, considerable variations on temperatures are seen. In contrast to our expectations, the temperature does not increase rapidly at the inlet of the nozzle, but it appears in the last vortex region behind the last baffle.
b) At a constant bs, increasing bc does not cause considerable increase of temperature.
c) By increasing the number of baffles, the temperature of fluid inside the shell increases.
d) The temperature rise after the third baffles is periodic, which is in good agreement with

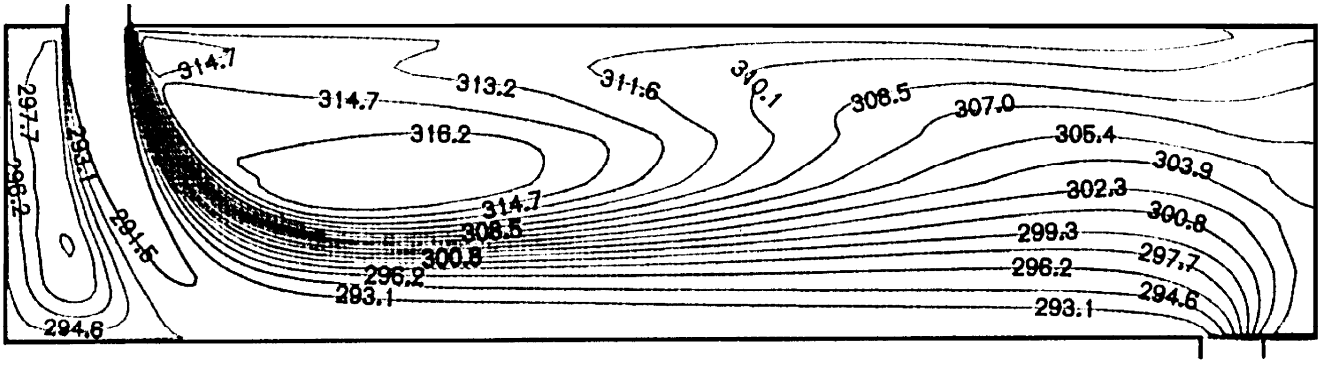

A

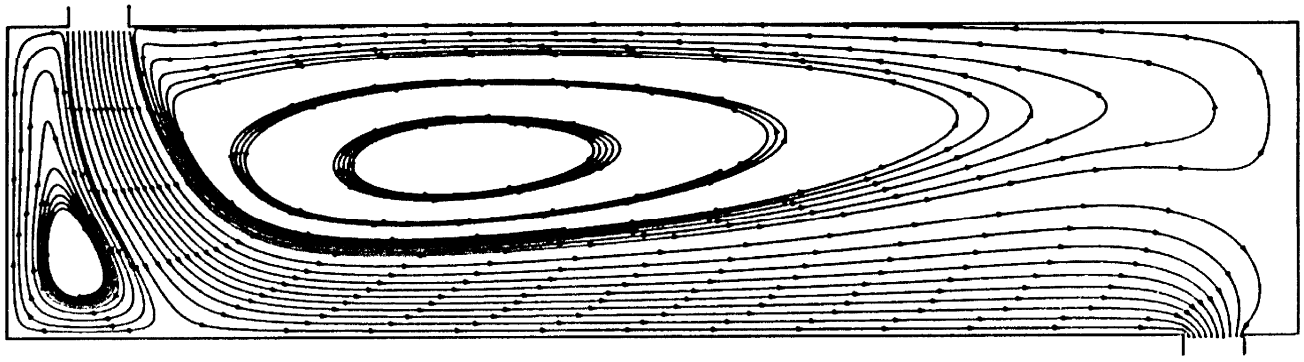

B

Figure 6. A - Stream line of exchanger without baffle and **B** - Isothermal lines of exchanger without baffle.

the experimental results and the other numerical work [17].

Effect of Baffles on Reynolds Number By definition, the Reynolds number inside the shell, according to the following relation, depends on the number of baffles [18].

$$Re = \frac{D_h G}{m} \qquad G = \frac{W}{a} \qquad a = \frac{ID_s * C\text{Å} * bc}{P_T}$$

It can be seen that Re does not depend on the percentage of baffle cut. Therefore, to increase the heat transfer conefficient through changing Reynolds number, the most appropriate solution is to increase the number of baffles. Figure 10 is a plot of the variation of Reynolds number versus the number of baffles for entry velocities. It can observes that by increasing the number of baffles the flow becomes turbulent more easily and with less cost compared with increasing the entrance velocity.

Variation of Nusselt Number and Pressure Drop The variation of dimensionless Nusselt number versus baffle spacing for constant baffle cut is indicates in Figure 11. In this figure, it can be seen that with increasing baffle spacing the dimensionless Nusselt number is decreased. Also in bc> 34% and bc< 0.45 the increase of dimensionless Nusselt number is very sharp. This phenomenon is the result of fields of vortex that appear between the repetitive lattice at the top and bottom.

Figure 12 shows the effects of the baffle spacing and the baffle cut on the shell-fluid dimensionless pressure drop. It can be seen that increasing the baffle spacing or baffle cut increases the pressure drop. This is in accord with the experimental measurements of the present work.

CONCLUSIONS

In the previous numerical analyses [5,6], a repetition of an identical geometrical module of the exchanger has been studied as a domain of calculation. While in this research, as a new approach in current numerical analysis, entire geometry to shell-and-tube heat exchanger including entrance and exit regions were considered as a domain of calculation. Experimental and numerical results have been compared over a wide range of Reynolds numbers (1,000 to 1,000,000). The most important results of this research are as follows:

1. Using a combination of the experimental and numerical methods, it would be possible to study heat and flow rate in shell-side even further.
2. Comparison of temperature profile of exchanger, with and without baffles, shows that baffles have the vital role in heat transfer rate.
3. The results also show that the effect of changing the number of baffles is more

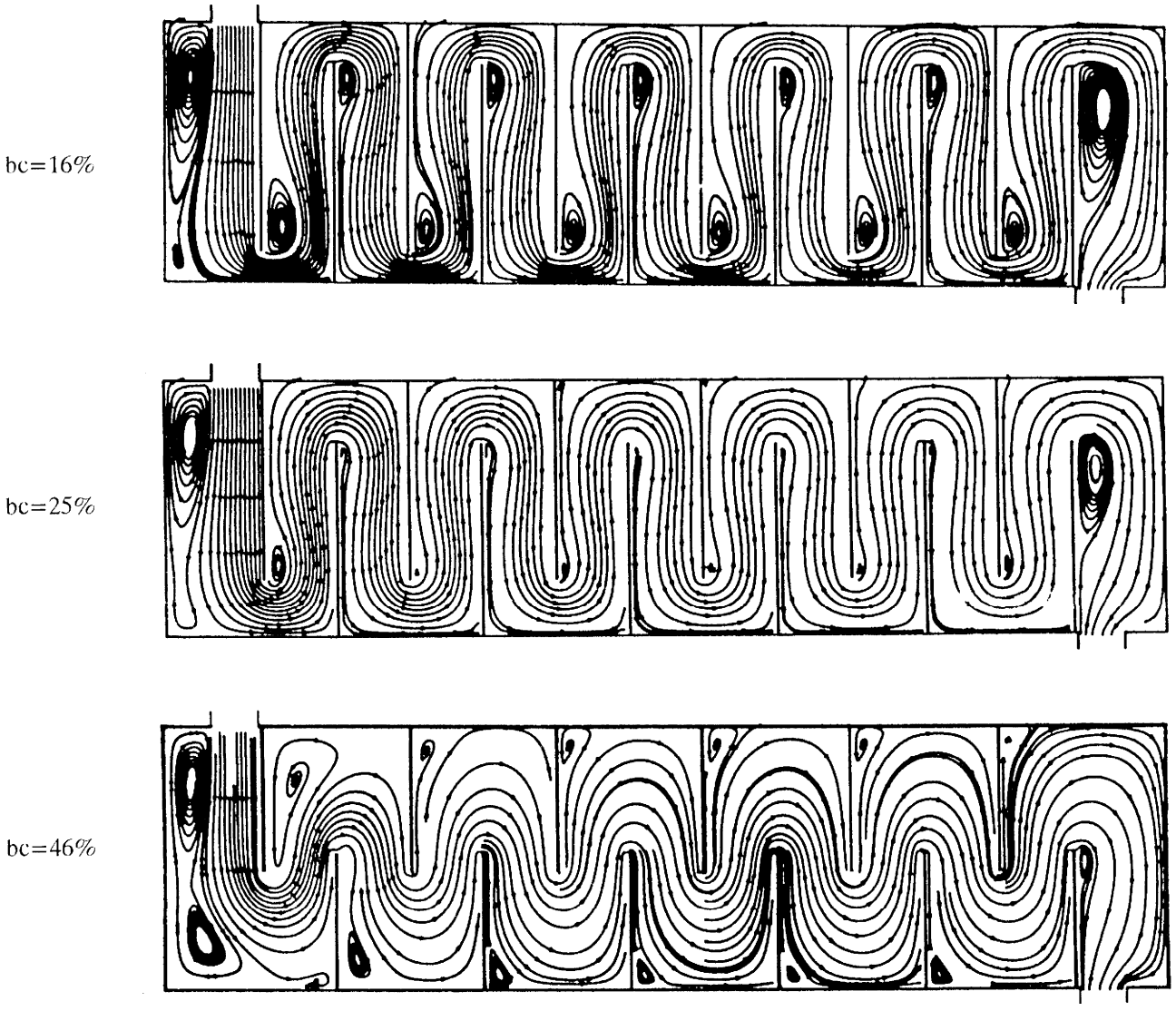

Figure 7. Stream lines for constant baffle spacing bs=0.33.

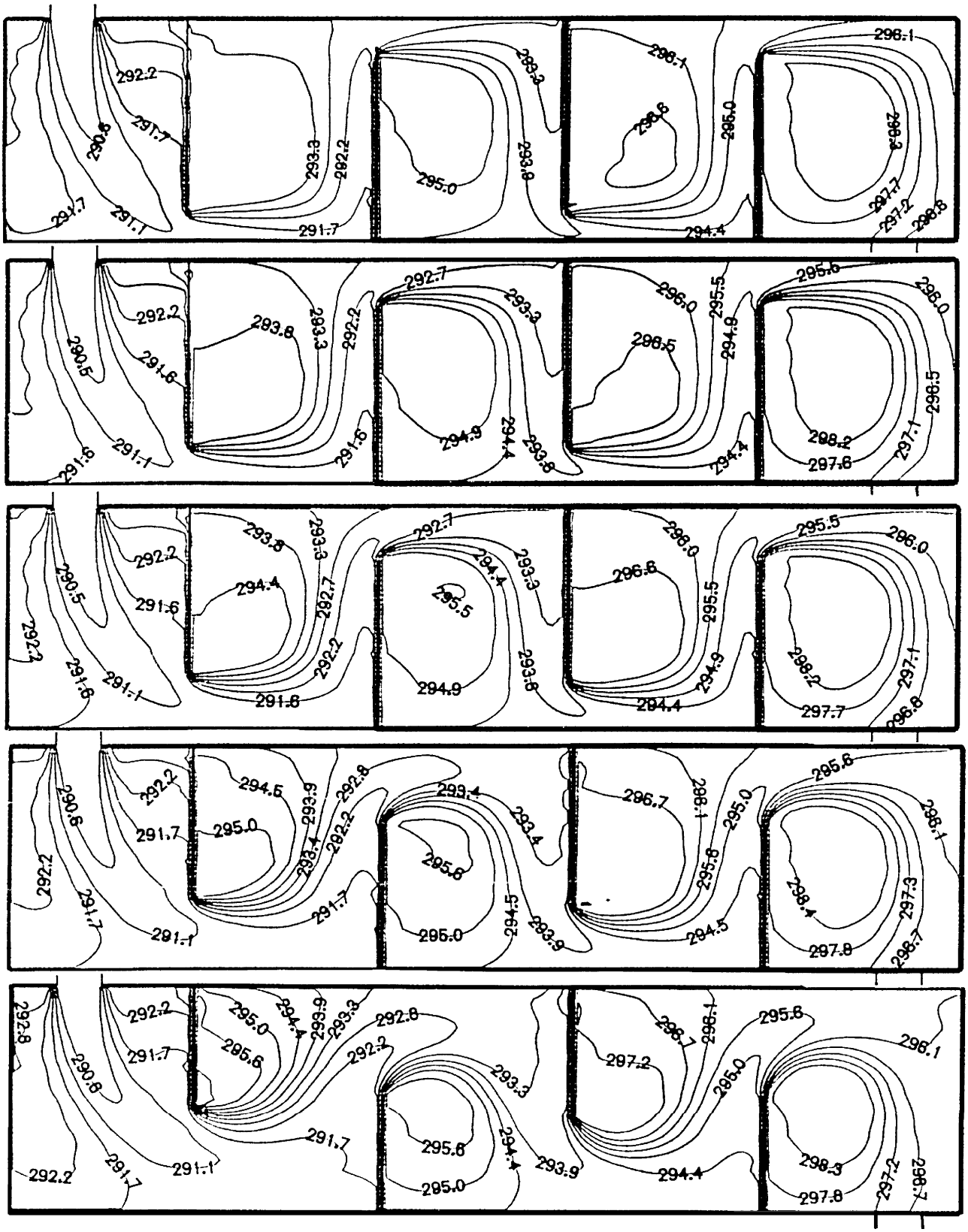

Figure 8. Isothermal lines for constant baffle spacing bs=1.0.

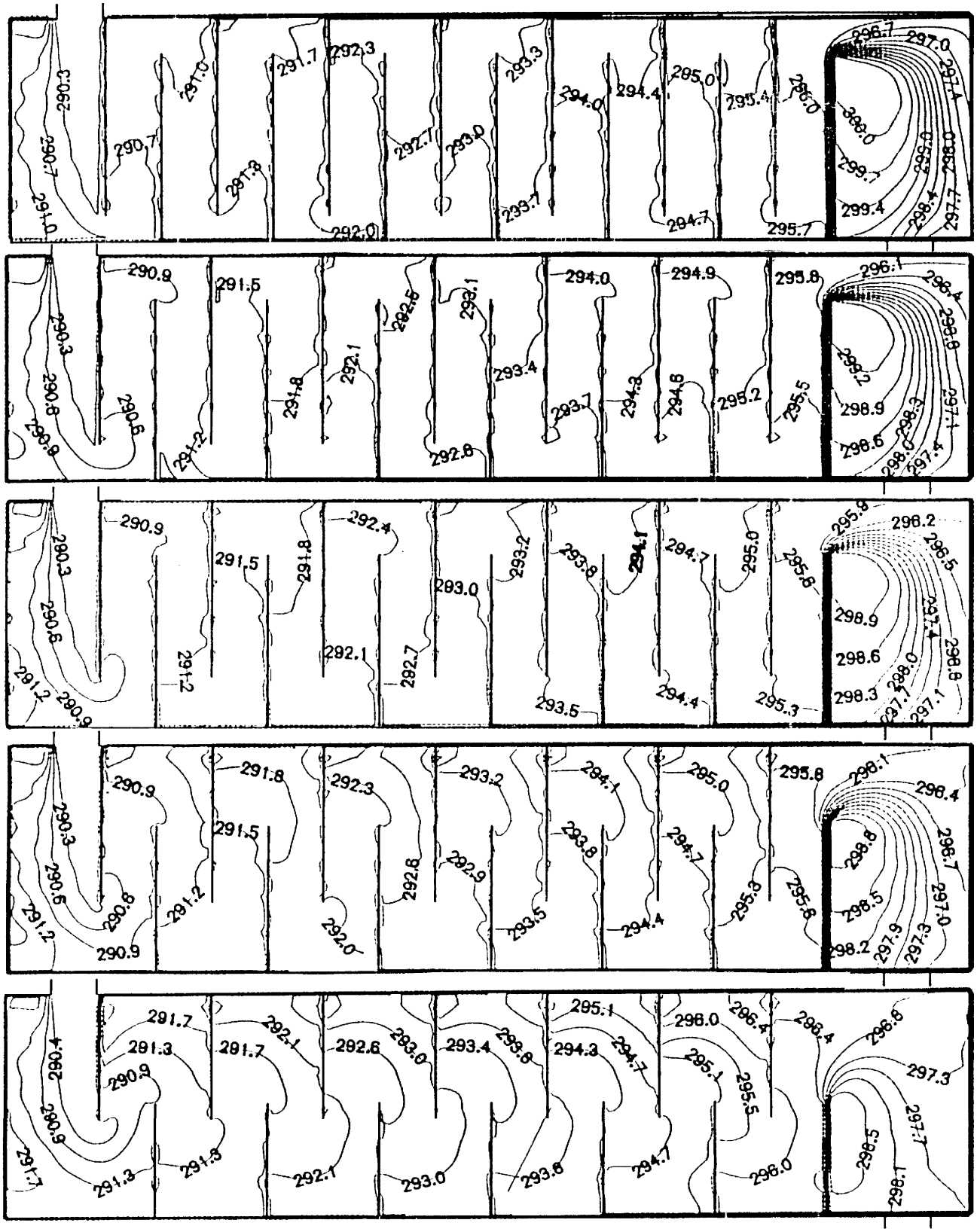

Figure 9. Isothermal lines for constant baffle spacing bs=0.20.

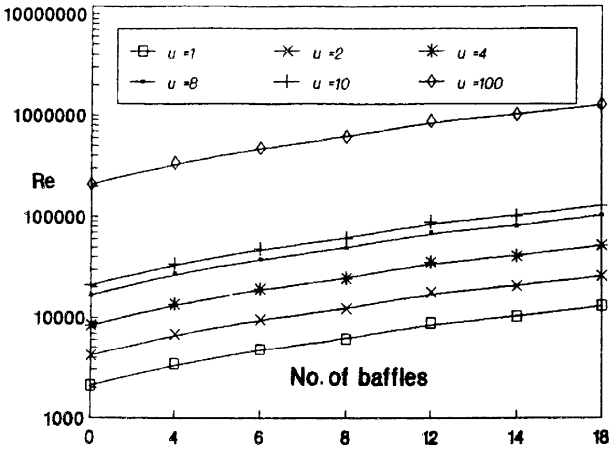

Figure 10. Reynolds number curve for inlet constant velocity.

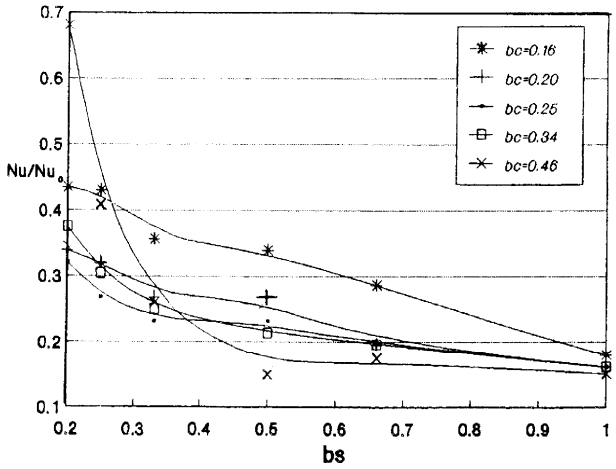

Figure 11. Dimensionless Nusselt number for constant baffle cut.

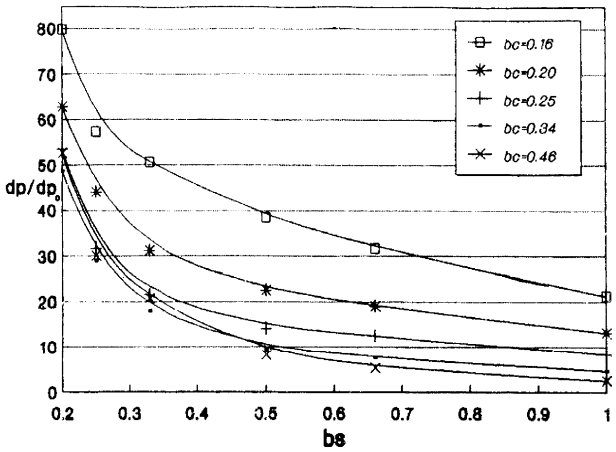

Figure 12. Dimensionless Pressure drop for constant baffle cut.

important than varying the height of baffles for heat transfer rate inside the shell.

4. The temperature rise after the third baffles is periodic.
5. Increasing Reynolds number in shell-side causes the increase of heat transfer rate. Reynolds number can be increased by adding the number of baffles more easily and with less cost as compared to increasing the inlet velocity of the fluid.
6. Increasing the dimemsionless Nusselt number is very sharp for bc> 34% and bs<0.45.

NOMENCLATURE

a	[m^2]	flow area across tube bundle
bs	[m]	baffles spacing
D_h	[m]	hydraulic diameter
G	[kg/s. m^2]	mass velocity
h	[W/m^2.°C]	heat transfer coefficient
J_h		dimensionless heat transfer
L	[m]	rube length
N		total number in heat exchanger
OD_t	[m]	tube length
pr		Prandtl number
Re		Reynolds number
S		source terms
v	[m/s]	shell-fluid radial velocity
r	[m/s]	shell-fluid velocity
e		dissipation of kinetic energy
f		dependent variable
A	[m^2]	heat exchanger area
CÅ	[m]	clearance between tube
f_x		axial-flow friction factor
G_{max}	[kg/s.m^2]	radial or circumferential mass flow rate based on minimum free area
m		tube pass
p	[kg/m^2]	Pressure
q	[W]	heat duty
R_r		distributed resistance of tubes in radial direction
t	[m]	shell thickness
x		axial coordinate
m	[kg/m.s]	viscosity
G		exchange factor

	baffle cut
[m]	baffle diameter
	radial-flow friction factor
[m]	shell inside diameter
[m]	tube inside diameter
[m^2/s^2]	turbulence energy
	shell pass
[m]	tube pitch
	radial coordinate
	distributes resistance of tubes in axial direction
[m/s]	shell-fluid axial velocity
[kg/m^3]	mass flow rate
	porosity (fluid volume/total volume)

REFERENCES

1. Butterworth, D. and Moscone, S. F., "Heat transfer heads into the 21st century", ***Chem. Eng. Prog.***, (Sep. 1991).
2. Tinker, T., "Shell side characteristic of shell-and-tube heat exchangers", Parts I, II and III. General discussion of heat transfer, ***Proc. Instn. of Mech. Eng.***, London, (1951).
3. Patankar, S. V. and Spalding, D. B., "A calculation procedure for the transient and steady-state behavior of shell and tube heat exchangers", IMPERIAL COLLEGE, (1972).
4. Patankar, S. V. and Spalding, D. B., "A calculation procedure for heat and momentum transfer in three dimensional Parabolic flow", ***Int. J. Heat & Mass Transfer***, Vol. 15, p. 1787, (1927).
5. Choi J. M. and Anand N. K., "Heat transfer in a serpentine channel with a series of right-angle turns", ***Numerical Heat Transfer***, part A, Vol. 23, pp. 189-210, (1993).
6. Kelkar K. M. and Patankar S. V., "Numerical prediction of flow and heat transfer in a parallel plate channel with staggered fins", ***Journal of Heat Transfer***, Vol. 109, (1987).
7. Noie Baghban, S. H., "Design and construction of a chemical reactor under pressure with stirrer", ***Second Chemical Engineering Conference***, Amirkabir Uni., Tehran pp. 84-89, (1996).
8. Kern, D. Q., "Process heat transfer", McGraw-Hill, (1950).
9. Standard of Tubular Exchanger Manufacture Association (TEMA), (1992***).***
10. Patankar, S. V. and Spalding, D. B., "Computer analysis of the three-dimensional flow and heat transfer in a steam generator", ***Forsch. Ing-wes***, 44, (1978).
11. Chen, Q., "Comparison of different k-e models for indoor air flow computations", ***Numerical Heat Transfer***, Part B, 353-369, (1995).
12. Moghiman, M., "Numerical Predictions of the carbon burnout performance of coal-fired non-slagging cyclone combustors", ***Journal of the Institute of Energy***, 69, pp. 31-38, (1996).
13. Rodi, W., "A new algebraic relation for calculating the Reynolds stresses", ***ZAMM 56***, p. 219, (1976).
14. Launder, B. E. and Splading, D. B., "The numerical computation of turbulent flows", ***Computer Methods in Applied Mechanics and Engineering*** 3, pp. 269-289, (1974).
15. Patankar, S. V., "Numerical heat transfer and fluid flow", McGraw-Hill, (1980).
16. Bell, K. J., "Final report of the cooperative research program on shell and tube heat exchangers", University of Delaware Eng. Exp. Stat. Bulletin 5 (1963).
17. Fukai, J. and Miyatake, O., "Laminar-flow heat transfer within parallel-plate channel with staggered baffles", ***Heat transfer, Japanese research***, 22 (2), (1993).
18. Ludwig, Ernest E. "Applied design for chemical and petrochemical plants", Vol. 3, Gulf Publishing Co., (1983).